NiO nanoparticles electrodeposited on reduced GO–CuO nanocomposite bulk modified CCE as a sensitive glucose sensor

Habib Razmi ✉, *Hossein Shirdel, Rahim Mohammad-Rezaei*

Electroanalytical Chemistry Research Laboratory, Faculty of Sciences, Azarbaijan Shahid Madani University, P.O. Box: 53714-161 Tabriz, Iran
✉ *E-mail: h.razmi@azaruniv.edu.com*

Published in Micro & Nano Letters; Received on 22nd September 2016; Revised on 16th November 2016; Accepted on 24th November 2016

A novel enzymeless glucose sensor based on nickel oxide (NiO) nanoparticles electrodeposited on reduced graphene oxide–copper oxide nanocomposite bulk modified carbon ceramic electrode (rGO–CuO/CCE) was reported. The prepared NiO/rGO–CuO/CCE was characterised by scanning electron microscopy, energy-dispersive X-ray spectroscopy, atomic-force microscopy, electrochemical impedance spectroscopy (EIS) and cyclic voltammetry techniques. Electrocatalytic performance of the NiO/rGO–CuO/CCE was investigated in details for the electro-oxidation of glucose using cyclic voltammetry and amperometry techniques. The developed sensor responds efficiently to glucose over the concentration range 5–920 μM with the detection limit 2.63 μM and sensitivity 5980 μA mM^{-1} cm^{-2}. According to EIS studies, ternary presence of rGO, CuO and NiO nanoparticles increased the electron transfer performance and sensitivity of NiO/rGO–CuO/CCE to glucose. The prepared sensor was applied for the determination of glucose in human serum samples with satisfactory results. Owing to renewable and polishable surface, high sensitivity, reproducible responses and long-term stability, the developed sensor could be used in clinical applications.

1. Introduction: Over the past decades there has been a lot of interest in the development of new sensors and biosensors for glucose monitoring. Owing to the difficulties and limitations in the use of glucose oxidase in biosensors, considerable attention had been paid to develop non-enzymatic electrodes [1, 2]. Previous studies have focused on the use of noble metals as well as their alloy electrodes as non-enzymatic glucose sensors [3]. Since the use of these metals is very costly, considerable research has been concentrated on the use of more affordable metal oxide materials such as nickel oxide (NiO), copper oxide (CuO) and cobalt oxide [4–7]. Owing to high surface area, good biocompatibility, relatively low cost and high catalytic activity, NiO and CuO can be ideal modifying agents for non-enzymatic glucose monitoring.

Recently, graphene and its derivate materials have been proposed to design higher electrochemical performance sensors [8–10]. Nanocomposites of metal-graphene and metal oxide–graphene are expected to be an important class of materials in the area of nanotechnology [11]. The performance of hybrid nanostructured materials mainly depends on their size, morphology, composition, structure and crystal phases [12–14].

Surface modification of electrodes with graphene via coating and electrodeposition techniques are the most frequently used methods. These methods show some limitations including non-reproducible results, time consuming and high costs. Graphene paste electrodes and sol–gel derived electrodes are another class of graphene-based modified electrodes which could be bulkily modified and thus are polishable and renewable. Graphene paste electrodes are suffered from weak mechanical stability and low reproducibility. Sol–gel derived ceramic composite electrodes (CCEs) are a new class of renewable electrodes which graphite, graphene, metals and metal oxides could be doped into sol–gel matrix during the hydrolysis of alkoxy silane and gelation process [15, 16].

Here, reduced graphene oxide/CuO nanocomposite (rGO–CuO) was perpetrated by a homogeneous co-precipitation method. Afterwards, rGO–CuO and graphite powder were trapped into the sol–gel matrix to result rGO–CuO/CCE. Then, NiO nanoparticles were electrodeposited on the rGO–CuO/CCE. The prepared NiO/rGO–CuO/CCE was investigated in details for the electro-oxidation of glucose. The modified electrode shows excellent stability, reproducibility and appropriate analytical figure of merits. The developed sensor has been successfully used for determination of glucose in human serum samples.

2. Experimental

2.1. Reagents and chemicals: All chemicals employed in this work were of analytical reagent grade and used without further purification. High purity graphite powder was from Merck. Ethyltrimethoxysilane was purchased from Fluka. Glucose, Ni nitrate, potassium permanganate ($KMnO_4$) and other reagents were of analytical grade from Merck. The fresh human serum samples were found from clinical laboratory. All solutions were prepared with doubly distilled water.

2.2. Instruments: Scanning electron microscopy (SEM, LEO 440i, Oxford, UK) was used in conjunction with energy-dispersive X-ray spectroscopy (EDS) to study the morphology and composition of the NiO modified rGO–CuO/CCE. The electrochemical experiments were carried out using an AUTOLAB PGSTAT-100 (potentiostat/galvanostat) equipped with an USB electrochemical interface and driven by a GPES 4.9 software package (Eco Chemie, The Netherlands). A three-electrode cell system composed of a saturated (KCl 3 M) calomel electrode (SCE) as the reference electrode, a platinum wire as the auxiliary electrode and the prepared NiO/rGO–CuO/CCE ($d = 1$ mm) as the working electrode were employed for the electrochemical studies.

2.3. Synthesis of GO: GO was prepared from purified natural graphite using the modified Hummers–Offeman method [17], where graphite powder (5 g) was added to 100 ml of 98% sulphuric acid in an ice bath. Then, sodium nitrate (2.5 g) was added to the solution and lastly $KMnO_4$ (15 g) was gradually added while stirring. The stirring was continued for 2 h at temperatures below 10°C, followed by 1 h at 35°C. At this point, the sample became paste-like and 250 ml of de-ionised water was added to the mixture in an ice bath. Once the effervescence stopped, the sample became an orange yellow colour and the

temperature of the mixture was increased to 98°C and held for 10 min before the mixture was cooled to room temperature. Next, 50 ml hydrogen peroxide was added to the mixture, heated to 90°C and held for 30 min. The resultant mixture was centrifuged and washed several times with boiling water until the pH of the supernatant became neutral. Finally, the resulting solid was dried at 60°C for 24 h.

2.4. Preparation of rGO–CuO nanocomposite: The rGO–CuO nanocomposite was prepared by homogeneous co-precipitation and then subsequent reduction with hydrazine (N_2H_4). In a typical experiment, 5 mmol $CuCl_2$ was dissolved in 50 ml water, 150 mmol urea was dissolved in another 50 ml water, then urea and $CuCl_2$ solutions were slowly and sequentially added to 50 ml of 2 mg ml^{-1} GO suspension under stirring. After exposure to ultrasound from an ultrasonic bath for 30 min, the mixture was heated at 90°C for 1.5 h. When cooled to room temperature, 0.5 ml N_2H_4 was added to the mixture while it was stirred. Then the mixture was refluxed at 100°C for 24 h in an oil bath, during which the mixture colour changed from black–brown to black. Then, the black mixture was collected by filtration. After washing with DI water to remove any excess N_2H_4 as well as other ions, the as-prepared product was annealed at 400°C for 3 h under an atmosphere of nitrogen in order to obtain an rGO–CuO nanocomposite.

2.5. Preparation of the CCE and rGO–CuO bulk modified CCE: Preparation of the CCE described by Lev and coworker by mixing 0.6 ml ETMOS, 0.9 ml methanol and 0.6 ml hydrochloric acid (0.1 M) [16]. This mixture was magnetically stirred for 30 min, after which 0.3 g graphite powder was added and the resultant mixture shaken for additional 1 min. A 5 mm length of a 2 mm inner diameter teflon tube was filled with the sol–gel carbon (C) mixture and dried under ambient conditions (25°C) for 48 h.

Fabrication of the rGO–CuO nanocomposite modified CCE (rGO–CuO/CCE) is described as follows. A solution of 0.6 ml methanol, 0.9 ml ETMOS and 0.6 ml hydrochloric acid (0.1 M) was mixed and stirred for 30 min to ensure uniform mixing, then 0.3 g graphite powder containing 30 mg rGO–CuO was added and the mixture was shaken for an additional 3 min. The mixture was added to a teflon tube and dried for 48 h at room temperature. The surface of rGO–CuO/CCE was polished and washed with de-ionised water and put in 0.05 M NaOH solution. Finally, the potential was scanned under the potential range between 0 and 0.8 V for 40 cycles at the scan rate of 100 mV s^{-1} in order to allow the Cu nanoparticles to be oxidised into CuO [18, 19].

2.6. Electrodeposition of NiO nanoparticles on rGO–CuO/CCE: Ni nanoparticles were deposited onto rGO–CuO/CCE from an aqueous solution containing 0.01 M $NiSO_4$ and 0.1 M KNO_3 by cyclic voltammetry [20]. The potential was scanned between −1 and 0.8 V for 65 cycles at a scan rate of 25 mV s^{-1} (Fig. 1). Then, the obtained Ni modified rGO–CuO/CCE was put in 0.05 M NaOH solution, and the potential was scanned under the potential range between −0.3 and 0.7 V for 40 cycles at a rate of 100 mV s^{-1} in order to allow the Ni to be oxidised into NiO (Fig. 2). During the electrodeposition, redox peaks were grown due to transition of Ni to NiO nanoparticles. The cathodic peak was attributed to the electrochemical reduction of Ni(III) and the anodic compartment is ascribed to the oxidation of Ni(II) as follows

$$Ni(OH)_2 + OH^- \rightleftarrows 2NiOOH + H_2O + e^- \quad (1)$$

The persistent increase of the peak currents with successive potential scans indicated that the activation of NiO has indeed been achieved. Consequently, the thickness of NiO film was growing by each cycle. The thickness of NiO depends on the numbers of scanned potential cycles (inset of Fig. 2). As can be seen, after 40 cycles the voltammetric currents reached to a steady state proving the maximum transition of Ni to NiO nanoparticles. After the deposition step, the modified electrode was washed thoroughly with de-ionised water and stored at room temperature.

3. Results and discussion

3.1. Characterisation of NiO/rGO–CuO/CCE: The morphology and composition of NiO nanoparticles modified rGO–CuO/CCE was studied by SEM, atomic-force microscopy (AFM) and EDS techniques. Fig. 3*a* shows the SEM images of rGO–CuO/CCE and NiO/rGO–CuO/CCE. As can be seen, NiO nanoparticles are well distributed on the rGO–CuO/CCE. In addition AFM micrograph of NiO/rGO–CuO/CCE (Fig. 3*b*) confirms three-dimensional (3D) and porous structure of NiO nanoparticles electrodeposited on the electrode surface. Also, due to porosity of electrode, the attachment of NiO nanoparticles were enhanced which confirms the suitability of rGO–CuO/CCE for deposition. The average size of NiO nanoparticles is ∼52 nm. The EDS spectrum of NiO/rGO–CuO/CCE is illustrated in Fig. 3*c*, in which the peaks of C, oxygen, Cu, silicon and Ni are pronounced. According to this analysis, ternary presence of Cu, Ni and C (rGO) could be seen on the electrode surface. The small size and homogeneous distribution of CuO nanoparticles and NiO could result advantageous such as large surface area, good catalytic activity and large number of active sites. All of these features lead to improvement in stability and sensitivity of NiO/rGO–CuO/CCE toward the glucose oxidation.

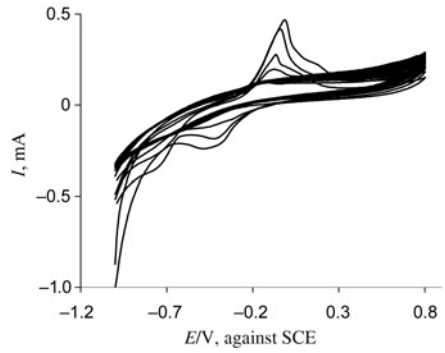

Fig. 1 *CVs of rGO–CuO/CCE in 0.01 M $NiSO_4$ and 0.1 M KNO_3; scan rate 25 mV s^{-1}*

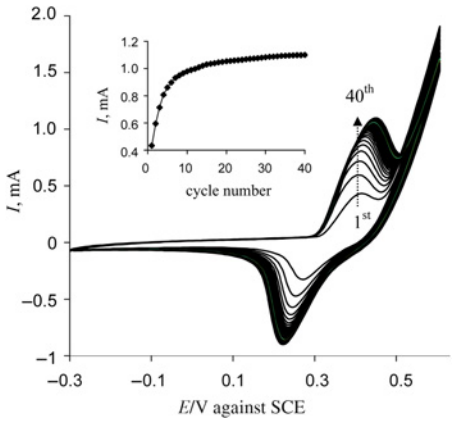

Fig. 2 *Electrodeposition and activation of NiO nanoparticles on rGO–CuO/CCE in 0.05 M NaOH solution; scan rate 100 mV s^{-1}*

doi: 10.1049/mnl.2016.0566

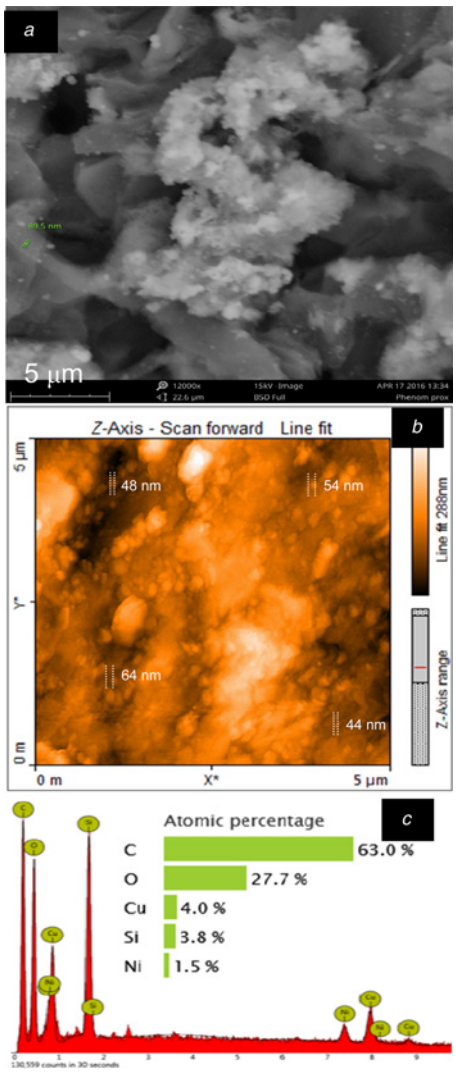

Fig. 3 *Characterisation of NiO/rGO–CuO/CCE*
a SEM image of rGO-CuO/CCE
b, *c*, AFM and EDS obtained for the NiO/rGO-CuO/CCE, respectively

3.2. Electrochemical impedance spectroscopy (EIS) studies: EIS is a helpful technique providing detailed information on the impedance changes of the electrode interface. In a typical impedance spectrum, a semi-circle part at higher frequencies

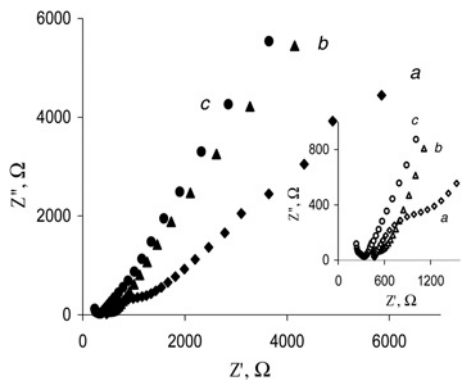

Fig. 4 *Main panel: the Nyquist plots of CCE (curve a), rGO/CCE (curve b) and rGO–Cu/CCE (curve c). Inset: the initial parts of Nyquist plots with more clarity*

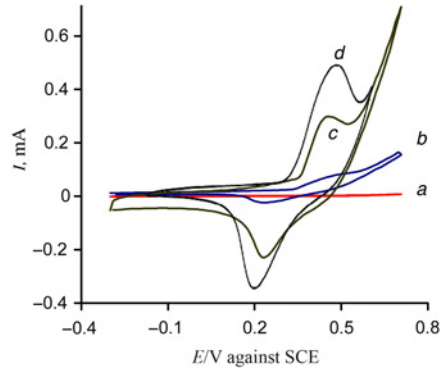

Fig. 5 *CVs of CCE (curve a), NiO/CCE (curve b), NiO/rGO/CCE (curve c) and NiO/rGO–CuO/CCE (curve d) in 0.1 M NaOH solution; scan rate 50 mV s^{-1}*

corresponds to the electron transfer-limit process and diffusion-limit process, respectively. The charge transfer resistance (Rct) can be estimated by the semi-circle diameter of the impedance spectra at high frequency.

Herein, EIS was employed to investigate the Rct of $Fe(CN)_6^{3-/4-}$ as a redox probe at the surface of CCE, rGO/CCE and rGO-Cu/CCE. Fig. 4 shows the Nyquist plots of the electrodes in 5 mM $Fe(CN)_6^{3-/4-}$ containing 0.1 M KNO_3 as the supporting electrolyte. According to this Letter, CCE showed a semi-circle-like plot with large Rct value (curve *a*). The Rct value of redox probe was decreased after doping rGO to CCE (rGO/CCE) structure (curve *b*) confirming that rGO facilitated the electron transportation at the electrode surface due to its high conductivity. The Rct value was highly decreased after the modification of CCE with rGO–CuO nanocomposite due to the deposition of highly conductive CuO nanoparticles on rGO sheet. This confirms that CuO nanoparticles were well-separated on the rGO surface. Therefore, rGO–CuO acted as an excellent electronic substrate with high electron transfer passages.

3.3. Electrochemical properties of modified electrodes: Fig. 5 shows the cyclic voltammograms (CVs) of CCE (curve *a*), NiO/CCE (curve *b*), NiO/rGO/CCE (curve *c*) and NiO/rGO–CuO/CCE (curve *d*) in 0.1 M NaOH solution at the scan rate of 50 mV s^{-1}. As can be seen, there is no redox peak at the CCE. However, a weak anodic and cathodic peak was appeared for NiO/CCE. After addition of rGO to CCE structure, the fabricated NiO/rGO/CCE

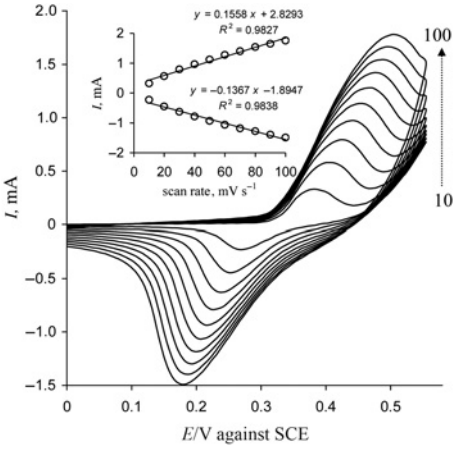

Fig. 6 *CVs of NiO/rGO–CuO/CCE in 0.1 M NaOH, at different scan rates (10, 20, 30, 40, 50, 60, 70, 80, 90 and 100 mV s^{-1}. Inset shows the dependence of the anodic and cathodic peak currents on the scan rate of potential*

represented an appropriate redox peak which could be due to the presence of high conductive rGO in the electrode structure (curve *c*). The positive role of CuO in the electron transfer performance of NiO/rGO–CuO/CCE was clearly shown in the last curve (curve *d*). As can be seen, the redox currents were remarkably enhanced in comparison with NiO/rGO/CCE and NiO/CCE. These results prove the constructive function of rGO–CuO nanocomposite in the NiO/rGO–CuO/CCE structure and also well distribution in CCE structure as a suitable nanocomposite.

Fig. 6 shows the CVs of the NiO/rGO–CuO/CCE at different scan rates in 0.1 M NaOH. The linear dependence of the peak currents I_{pa} and I_{pc} on the scan rate of potential was obtained up to 100 mV s^{-1}. Ni(II)/(III) redox peak currents grew linearly with scan rate; this behaviour is what expected for surface redox reactions (inset of Fig. 6). The ratio of I_{pa}/I_{pc} remains almost equal to unity at different scan rates, as expected for surface-type behaviour.

3.4. Electrocatalytic oxidation of glucose: To represent the electrocatalytic performance of NiO/rGO–CuO/CCE, the electrode response was investigated in the presence of glucose.

For this purpose, CVs of NiO/rGO–CuO/CCE were conducted in different glucose concentrations in deoxygenated NaOH solution (pH 12) at the scan rate of 50 mV s^{-1}. Fig. 7 illustrates the CVs of the NiO/rGO–CuO/CCE in the absence (curve *a*) and the presence of 1-6 mM glucose.

With the addition of glucose, the anodic and cathodic currents were increased significantly which correspond to the oxidation and reduction of glucose on the surface of electrode. The similar experiments were examined with the use of CCE, rGO/CCE, NiO/CCE and NiO/rGO/CCE (not shown). According to these studies, CCE and rGO/CCE did not show any response to glucose oxidation. However, NiO/CCE and NiO/rGO/CCE show a weak response to glucose oxidation which was negligible in comparison with NiO/rGO–CuO/CCE. The enhanced electrocatalytic response of NiO/rGO–CuO/CCE could be due to high conductivity of rGO and CuO, uniform distribution of NiO on the surface of rGO–CuO/CCE and high surface to area ratio and porosity of the electrode.

For the electro-oxidation of glucose two different mechanisms were reported [21]: (i) adsorption of glucose on Ni(III) oxide active surface followed by electro-oxidation process. In this manner, glucose is directly oxidised by Ni(III) oxide as catalyst

$$\text{Ni(III)} - \text{glucose} \longrightarrow \text{Ni(III)} + \text{intermediate} \quad (2)$$

$$\text{Ni(III)} - \text{intermediate} \longrightarrow \text{Ni(III)} - \text{products} \quad (3)$$

(ii) Mediated oxidation mechanism involving the redox transition of Ni species from Ni(II) to Ni(III), where glucose oxidised on the modified surface via the following reaction according to the Fleischmann mechanism

$$\text{Ni(III)} + \text{glucose} \longrightarrow \text{intermediate} + \text{Ni(II)} \quad (4)$$

$$\text{Ni(III)} + \text{intermediate} \longrightarrow \text{products} + \text{Ni(II)} \quad (5)$$

In our Letter considering redox behaviour of Ni(III)/(II), the oxidation of glucose proceeds mainly according to the following reactions (6) and (7)

$$\text{Ni(II)} \longrightarrow \text{Ni(III)} + e^- \quad (6)$$

$$\text{Ni(III)} + \text{glucose} \longrightarrow \text{Ni(II)} + \text{glucolactone} \quad (7)$$

Therefore, when applying a potential of 0.5 V to the modified electrode, the Ni(III) species produces on the electrode surface and oxidises glucose to generate Ni(II) species, producing the glucolactone, simultaneously.

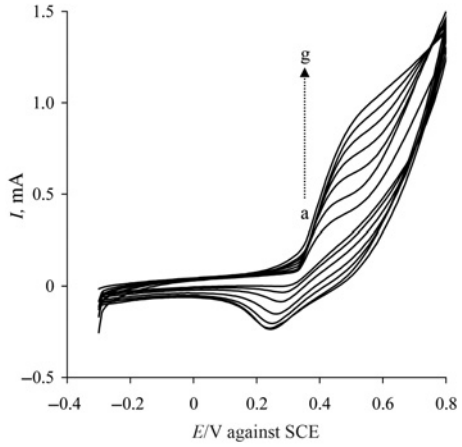

Fig. 7 *CVs of NiO/rGO–CuO/CCE in the absence (curve a) and the presence (b–g) of 1–6 mM glucose in 0.1 M NaOH solution; scan rate: 50 mV* s^{-1}

To show the highlight, the function of CuO and rGO in the electrode structure, and their importance in electrode sensitivity, amperometric responses of CCE, NiO/rGO/CCE and NiO/rGO–CuO/CCE were recorded in the presence of 50 µM glucose, in 0.1 M NaOH solution, applied potential of 0.5 V versus SCE and rotating speed of 1000 rpm (Fig. 8). According to this Letter, (a) CCE did not respond to glucose in analytical condition. (b) Comparison of NiO/rGO/CCE and (c) NiO/rGO–CuO/CCE responses to glucose show that the presence of CuO in the electrode structure has increased the sensitivity of electrode. Suitable distribution of CuO on rGO, porous and rigid morphology of CCE, and high active surface area of NiO nanoparticles on rGO–CuO resulted in a novel enzymeless glucose sensor with enhanced sensitivity and suitable stability.

3.5. Amperometric detection of glucose and analytical figure of merits of NiO/rGO–CuO/CCE: To obtain optimum conditions for amperometric determination of glucose in hydrodynamic systems, the hydrodynamic voltammogram of 2 mM glucose at the NiO/rGO–CuO/CCE over the potential range from −0.3 to 0.8 V was recorded. According to this Letter, the maximum current was obtained at the potential of 0.5 V [22]. Thus, a potential of 0.5 V was selected as the working potential for amperometric determination of glucose under hydrodynamic conditions. Fig. 9 shows a typical current–time response of the NiO/rGO–CuO/CCE in 0.1 M NaOH solution under the optimised conditions for the successive addition of glucose with 5 and 50 µM increments. As shown in this figure, a well-defined response was observed after each addition over the range 5–920 µM. It was observed that the

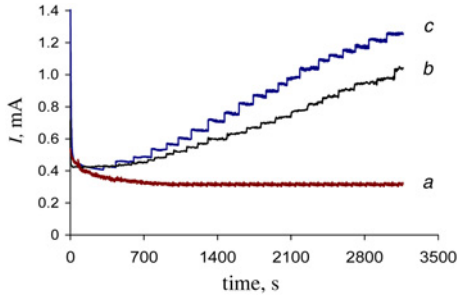

Fig. 8 *Amperogram of CCE, NiO/rGO/CCE and NiO/rGO–CuO/CCE in glucose in 0.1 M NaOH solution; applied potential 0.5 V versus SCE*

doi: 10.1049/mnl.2016.0566

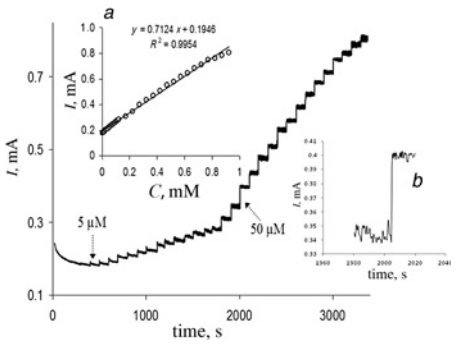

Fig. 9 *Hydrodynamic amperometric response of NiO/rGO–CuO/CCE to successive addition of glucose with 5 and 50 μM increments. Conditions: applied potential of 0.5 V versus SCE, 0.1 M NaOH solution and rotation speed of 1000 rpm*
a Inset shows the corresponding calibration curve
b Inset shows sensor response in the expanded time scale

sensor responds so rapidly to the glucose, as about 95% of the steady-state current is obtained within 5 s. The inset (a) of Fig. 9 shows the plot of electrocatalytic current versus glucose concentration. The linear regression equation of calibration curve is expressed as I (mA) = 0.7124C (mM) + 0.1946 with a correlation coefficient of 0.9954 (n = 30). Then, the sensitivity and limit of detection (LOD) were found to be 5980 μA mM^{-1} cm^{-2} and 2.63 μM (at signal-to-noise ratio of 3) respectively. Sensitivity, linear range and LOD of the fabricated electrode were compared with those of the previous reports and results were shown in Table 1. Comparable and/or better figure of merits of NiO/rGO–CuO/CCE suggested the electrode for routine and clinical applications.

3.6. Renewability and stability of the NiO/rGO–CuO/CCE: Owing to fouling, efficiency of electrodes usually decreases during the electrocatalytic processes. Thus, renewability of the electrodes surface would be considered as a criterion characteristic in electrochemical sensors. The renewability of the NiO/rGO–CuO/CCE was examined by amperometric technique in determination of glucose after several polishing steps. According to this Letter, amperometric responses of five independently polished and prepared NiO/rGO–CuO/CCE, under the same conditions, toward the electro-oxidation of 50 μM glucose showed appropriate reproducibility (relative standard deviation (RSD) of 2.7%).

Fast and high stable response of NiO/rGO–CuO/CCE toward the glucose is the extremely attractive feature of this Letter. The oxidation current of 50 μM glucose for a period of about 30 min under hydrodynamic conditions was investigated (not shown). The stability of electrode response demonstrated long-term applicability of the NiO/rGO–CuO/CCE for the determination of glucose. In this Letter, only 5% decrease in current was observed after 1800 s which could be attributed to the consumption of glucose at the surface of electrode due to its electro-oxidation reaction.

3.7. Interference study and determination of glucose in human serum sample: Under the optimal conditions for determination of glucose, interferences of some substances that exist in biological liquids were investigated. The interference tests were carried out by the amperometric technique in the presence of 50 μM glucose and the same concentrations of uric acid (UA), ascorbic acid (AA), dopamine (DA) and alanine. There was no obvious change in the glucose signal when these substances were added to the electrolyte solution (Fig. 10).

To verify the possibility of the NiO/rGO–CuO/CCE for glucose analysis, it was applied for the determination of glucose in blood serum sample. Five fresh blood samples were supplied by the Maku hospital (West Azarbaijan, Iran) and were centrifuged for 20 min at 12,000 rpm to separate out the serum, then diluted with 0.1 M NaOH before analysis.

Table 2 Analysis of glucose in blood serum samples

Samples	Diluted concentration, mM	Added, mM	Found, mM	Recovery, %	RSD % (n = 5)
1	0.31	3.0	3.52	106.3	4.8
2	0.60	3.0	3.45	95.83	3.43
3	0.80	3.0	3.86	101.57	4.54
4	1.24	3.0	4.01	102.55	3.18
5	1.63	3.0	4.54	94.57	3.95

Table 1 Figures of merit of some non-enzymatic glucose sensors

Electrode material	Sensitivity	Linear range	LOD, μM	Reference
PtM (M = Ru, Pd and Au) on CNTs-ILs[a]	10.6 μA mM^{-1} cm^{-2}	up to 15 mM	50	[23]
3D gold	46.6 μA mM^{-1} cm^{-2}	5×10^{-6}–10^{-2} M	3.2	[24]
Ni/aluminium layered double hydroxide	0.182 μA mM^{-1}	up to 10 mM	10	[25]
cobalt (II) phthalocyanine tetrasulphonate	5.695 μA mM^{-1}	0.25–20 mM	100	[26]
Ni-cobalt/rGO	1773.61 μA mM^{-1} cm^{-2}	10 μM–2.65 mM	3.79	[27]
NiO/rGO–CuO/CCE	5980 μA mM^{-1} cm^{-2}	5–920 μM	2.63	this work

[a] Carbon nanotubes-ionic liquid

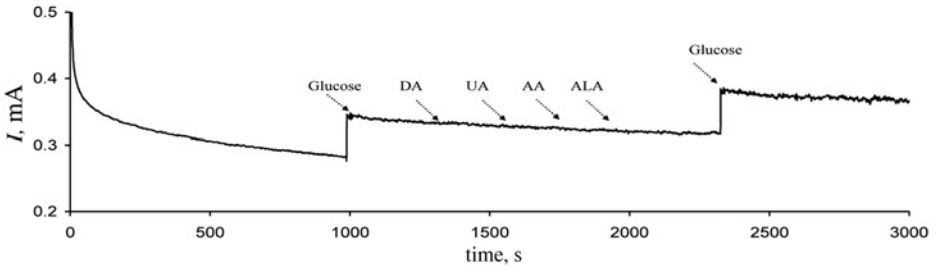

Fig. 10 *Interferences of some main organic molecules on the glucose signal. Concentration of DA, UA, AA and glucose was 50 μM*

Standard addition method was employed by adding pure glucose into the diluted real samples. The corresponding results are shown in Table 2. Statistical treatment of the data indicated that the method is accurate and credible. The recovery for the determination of glucose was ranged from 94.57 to 106.3 for the five samples which indicate the potential of the fabricated sensor in real sample analysis.

To evaluate the renewability of modified electrode, it was polished and re-coated with NiO particles for ten times at the same conditions, and the RSD value of 4.85% was calculated by measuring the anodic peak current. To study the long-term stability of the NiO/rGO–CuO/CCE, the CVs of the fabricated electrode were recorded after a period of 3 months in 0.1 M NaOH and 0.1 M NaCl at scan rate 50 mV s^{-1}. The decrease in peak current was negligible. Good reproducibility and stability of the NiO/rGO–CuO/CCE can be attributed to the porous nature of modifying layer and strong interaction between reduced GO and metal oxides nanoparticles.

4. Conclusion: In this Letter, a renewable non-enzymatic glucose sensor based on NiO nanoparticles electrodeposited on rGO–CuO bulk modified CCE was reported. Owing to high conductivity and high real surface area of rGO and CuO, the NiO/rGO–CuO/CCE showed higher electrochemical activity than the CCE, NiO/CCE and NiO/rGO/CCE. The low cost, easily fabricated, renewability, reproducibility and sensitive responses to glucose without enzyme loading resulted in a suitable biosensor for glucose determination in routine and clinical analysis.

5. Acknowledgment: The authors gratefully acknowledge the Research Council of Azarbaijan Shahid Madani University for financial support.

6 References

[1] Li Z., Chen Y., Xin Y., *ET AL.*: 'Sensitive electrochemical nonenzymatic glucose sensing based on anodized CuO nanowires on three-dimensional porous copper foam', *Sci. Rep.*, 2015, **5**, p. 16115
[2] Wang G., He X., Wang L., *ET AL.*: 'Non-enzymatic electrochemical sensing of glucose', *Microchim. Acta*, 2013, **180**, (3), pp. 161–186
[3] Tang J., Tang D.: 'Non-enzymatic electrochemical immunoassay using noble metal nanoparticles: a review', *Microchim. Acta*, 2015, **182**, (13), pp. 2077–2089
[4] Wang L., Zheng Y., Lu X., *ET AL.*: 'Dendritic copper-cobalt nanostructures/reduced graphene oxide-chitosan modified glassy carbon electrode for glucose sensing', *Sens. Actuators B, Chem.*, 2014, **195**, pp. 1–7
[5] Yu H., Jian X., Jin J., *ET AL.*: 'Nonenzymatic sensing of glucose using a carbon ceramic electrode modified with a composite film made from copper oxide, overoxidized polypyrrole and multi-walled carbon nanotubes', *Microchim. Acta*, 2015, **182**, (1), pp. 157–165
[6] Zhu X., Jiao Q., Zhang C., *ET AL.*: 'Amperometric nonenzymatic determination of glucose based on a glassy carbon electrode modified with nickel(II) oxides and graphene', *Microchim. Acta*, 2013, **180**, (5), pp. 477–483
[7] Chen H., Li C.-L., Li N., *ET AL.*: 'Facile synthesis of CuO–NiO nanocomposites with high surface areas and their application for lithium-ion batteries', *Micro Nano Lett.*, 2013, **8**, (9), pp. 544–548
[8] Ambrosi A., Chua C.K., Bonanni A., *ET AL.*: 'Electrochemistry of graphene and related materials', *Chem. Rev.*, 2014, **114**, (14), pp. 7150–7188
[9] Yavari F., Koratkar N.: 'Graphene-based chemical sensors', *J. Phys. Chem. Lett.*, 2012, **3**, (13), pp. 1746–1753
[10] Hu Z., Chen Y., Chen H.: 'Comparative study on the formation mechanism of graphene oxide-derived carbon/Pd composites', *Micro Nano Lett.*, 2011, **6**, (8), pp. 709–712
[11] Gao P., Liu D.: 'Facile synthesis of copper oxide nanostructures and their application in non-enzymatic hydrogen peroxide sensing', *Sens. Actuators B, Chem.*, 2015, **208**, pp. 346–354
[12] Gleiter H.: 'Nanostructured materials: basic concepts and microstructure', *Acta Mater.*, 2000, **48**, (1), pp. 1–29
[13] Kato K., Dang F., Mimura K.-I., *ET AL.*: 'Nano-sized cube-shaped single crystalline oxides and their potentials; composition, assembly and functions', *Adv. Powder Technol.*, 2014, **25**, (5), pp. 1401–1414
[14] Douvalis A.P., Bourlinos A.B., Tucek J., *ET AL.*: 'Development of novel FePt/nanodiamond hybrid nanostructures: L10 phase size-growth suppression and magnetic properties', *J. Nanopart. Res.*, 2016, **18**, (5), pp. 1–19
[15] Mohammad-Rezaei R., Razmi H., Jabbari M.: 'Graphene ceramic composite as a new kind of surface-renewable electrode: application to the electroanalysis of ascorbic acid', *Microchim. Acta*, 2014, **181**, (15), pp. 1879–1885
[16] Tsionsky M., Gun G., Glezer V., *ET AL.*: 'Sol-gel-derived ceramic-carbon composite electrodes introduction and scope of applications', *Anal. Chem.*, 1994, **66**, (10), pp. 1747–1753
[17] Hummers W.S., Offeman R.E.: 'Preparation of graphitic oxide', *J. Am. Chem. Soc.*, 1958, **80**, (6), pp. 1339–1339
[18] Shahrokhian S., Kohansal R., Ghalkhani M., *ET AL.*: 'Electrodeposition of copper oxide nanoparticles on precasted carbon nanoparticles film for electrochemical investigation of anti-HIV drug nevirapine', *Electroanalysis*, 2015, **27**, (8), pp. 1989–1997
[19] Razmi H., Nasiri H.: 'Trace level determination of hydrogen peroxide at a carbon ceramic electrode modified with copper oxide nanostructures', *Electroanalysis*, 2011, **23**, (7), pp. 1691–1698
[20] Ghanbari Kh., Babaei Z.: 'Fabrication and characterization of non-enzymatic glucose sensor based on ternary NiO/CuO/polyaniline nanocomposite', *Anal. Biochem.*, 2016, **498**, pp. 1–10
[21] Cao F., Guo S., Ma H., *ET AL.*: 'Highly sensitive nonenzymatic glucose sensor based on electrospun copper oxide-doped nickel oxide composite microfibers', *Talanta*, 2012, **101**, pp. 24–31
[22] El-Refaei S.M., Awad M.I., El-Anadouli B.E., *ET AL.*.: 'Electrocatalytic glucose oxidation at binary catalyst of nickel and manganese oxides nanoparticles odified glassy carbon electrode: optimization of the loading level and order of deposition', *Electrochim. Acta*, 2013, **92**, pp. 460–467
[23] Xiao F., Zhao F., Mei D., *ET AL.*: 'Nonenzymatic glucose sensor based on ultrasonic-electrodeposition of bimetallic PtM (M = Ru, Pd and Au) nanoparticles on carbon nanotubes–ionic liquid composite film', *Biosens. Bioelectron.*, 2009, **24**, (12), pp. 3481–3486
[24] Bai Y., Yang W., Sun Y., *ET AL.*: 'Enzyme-free glucose sensor based on a three-dimensional gold film electrode', *Sens. Actuators B, Chem.*, 2008, **134**, (2), pp. 471–476
[25] Ai H., Huang X., Zhu Z., *ET AL.*: 'A novel glucose sensor based on monodispersed Ni/Al layered double hydroxide and chitosan', *Biosens. Bioelectron.*, 2008, **24**, (4), pp. 1048–1052
[26] Özcan L., Şahin Y., Türk H.: 'Non-enzymatic glucose biosensor based on overoxidized polypyrrole nanofiber electrode modified with cobalt(II) phthalocyanine tetrasulfonate', *Biosens. Bioelectron.*, 2008, **24**, (4), pp. 512–517
[27] Wu M., Meng S., Wang Q., *ET AL.*: 'Nickel–cobalt oxide decorated three-dimensional graphene as an enzyme mimic for glucose and calcium detection', *ACS. Appl. Mater. Interfaces*, 2015, **7**, (38), pp. 21089–21094

doi: 10.1049/mnl.2016.0566